

H9/50

The Refractive Index of Air

Brian Schwartz, ECEN 5645, Fall 1999, Dr. Barnes

1. Motivation

For most photonics applications the refractive index of air can be neglected, that is, assumed to be unity. Hence, in optical path distance or refraction calculations, scientists and engineers do not, and need not, take into account how air's refractive index changes with temperature, pressure, and composition. As of 1965, knowing the value the refractive index of air, n , to eight decimal places satisfies most scientific applications [8].

Some applications do require this knowledge. Spectroscopy is done in air, so we need to know the refractive index where measurement is being taken to know absolute wavelengths, and hence, energies of atomic and molecular transitions.

Moore's Law states that the number of transistors on a semiconductor chip doubles every 18 months. This Law originated as a description, or perhaps a prediction. It is now a benchmark that chip manufacturers such as AMD, Motorola, and Intel use to set their goals [7]. How small a transistor can be written onto a chip limits how many of them can be written on a transistor.

Chip manufacturers use photolithography to write transistors on a chip. The principle behind lithography is as follows. Light (or an electron beam) is transmitted through a reticle (a mask) containing the pattern of the transistor to be written on the chip. A lens focuses this pattern onto the semiconductor+photoresist. Since the focused light has a pattern of the conducting parts of the reticle, it etches a pattern in the photoresist that matches the transistor [4].

Feature size on the circuit pattern is on the order of the wavelength of light used to etch them. These days 250 nm linewidths are made with a 248 nm KrF excimer laser. AMD, Motorola, and Intel are interested in making chips with 50 nm resolution. One method is a projection electron beam technology from Lucent called Scalpel. On this system, the mask and wafer stage positions need to be known quite accurately, as both of their positions are stepped in the x and y directions in the etching process. Laser interferometers monitor their positions to a 2.5 nm accuracy (See Figure 1, Appendix) [4]. The refractive index of air affects interferometer OPD, and hence position measurements, and Intel monitors air pressure to keep track of these changes [3a].

2. Two methods for measuring refractive index of air [3]

2.1. Fringe measurement in Fabry-Perot interferometer

The interference condition for light in the resonator is given by

$$2nd = \lambda_0(m + e). \quad (2-1)$$

n : refractive index of medium
 d : distance between two mirrors
 λ_0 : vacuum wavelength of light
 m : integer order of number of waves that fit in cavity.
 e : fractional order, = 0 on resonance.

To measure changes in refractive index, Eickhoff and Hall measured the fractional orders, e_1, e_2, \dots, e_i , by analyzing Fabry-Perot rings. For two such measurements, the change in refractive index is derived from (2-1). The fractional orders e_1 and e_2 are measured for the same integer order, m , so $m_1 = m_2$. Solving both expressions of their respective m and setting them equal to each other, we have

d will change with temperature

$$n_2 - n_1 \approx \frac{\lambda_0}{2d} (e_2 - e_1). \quad (2.2)$$

Mirror separation d can be considered constant over index change $n_2 - n_1$. Eickhoff and Hall cite a study that reports that for a full atmosphere, the "compressible étalon effect" is < 0.5 ppm/atm. Since the ambient pressure in the lab changes by a few percent (of an atmosphere) in the lab, this change can be ignored.

2.1.1 How to measure e_2 and e_1 [2]

The Fabry-Perot étalon consists of two parallel surfaces separated by a distance h with a medium index n' between them. For light wavelength λ_0 incident at an angle θ' to the étalon normal, the phase difference between a beam that is transmitted through the etalon with 0 internal reflections and one that escapes after one reflection off of each surface is

$$\delta = \frac{4\pi}{\lambda_0} n' h \cos\theta' + 2\phi, \text{ [See Appendix for derivation]} \quad (2.3)$$

where ϕ is the phase change upon internal reflection. For $n' > n$, the medium outside the etalon, $\phi = 0$, as there is no phase change upon reflection off a medium of lower index than the incident medium.

If a lens of focal length f images light exiting the etalon at points corresponding to their exit angle, interference maxima occur when the phase change is an integral multiple of 2π . If m is the m th interference maxima, then

$$m = \frac{\delta}{2\pi} = \frac{2\pi}{\lambda_0} n' h \cos\theta' + \frac{\phi}{\pi} \quad (2.4)$$

and

$$m\lambda_0 = 2n' h \cos\theta' + \lambda_0 \frac{\phi}{\pi} \quad (2.5)$$

The maximum value of m , m_0 , corresponds to interference of light incident normal to the etalon, i.e., $\theta' = 0$:

$$m_0 = \frac{2n' h}{\lambda_0} + \frac{\phi}{\pi} \quad (2.6)$$

$$m_0 \lambda_0 = 2n' h + \lambda_0 \frac{\phi}{\pi} \quad (2.7)$$

Consider the case where m_0 is not an integer. This means that the étalon's optical path $n'h$ does not equal an integer number of half-wavelengths:

$$m_0 = m_1 + e, \quad (2.8)$$

where m_1 is the integral order of the 1st bright fringe (closest to the center), and $e (<1)$, is the *fractional order at the center*. For the p th bright fringe, (2.5) becomes

$$m_p \lambda_0 = [m_1 - (p-1)]\lambda_0 = 2n' h \cos\theta_p + \lambda_0 \frac{\phi}{\pi}, \quad (2.9)$$

where $m_p = [m_1 - (p-1)]$ is the interference order. So if $p=1$, then $m_p = m_1$, and is the first interference order.

Upon substituting $m_1 = (m_0 - e)$ from (2.8) and solving for m_0 in (2.7), we have

$$2n' h(1 - \cos\theta_p) = (p-1 + e)\lambda_0. \quad (2.10)$$

From this expression we can determine e from the other measurable parameters in the lab. Using (2.2),

$$n_2 - n_1 \approx \frac{\lambda_0}{2d}(e_2 - e_1)$$

we can measure two values of e for different refractive indices (of air) between the FP plates, and find the refractive index difference.

2.1.2 To measure an absolute value of refractive index n_2 :

If we want to measure the value of the refractive index of the air, say, in our lab, n_2 , relative to that in vacuum, $n_1 = 1$, we need to know the following parameters in vacuum:

1. laser wavelength λ_0 in vacuum
2. integer order, m .
3. mirror separation, d

Determining λ_0 and m allows us to determine, by applying (2.1) to the vacuum resonance condition ($n=1$, $e=0$), that

$$d = \lambda_0 m / 2. \quad (2.1.2-1)$$

Laser wavelength is determined by comparison with an I₂-stabilized laser [11]. Use of the method of exact fractions can determine the integer order m [5].

2.1.3 How to measure fractional orders: a conceptual outline

Eickhoff and Hall's Fabry-Perot refractometer consists of the output of a stabilized He-Ne laser coupled into a single mode fiber (Figure 2.1-3, Appendix). The collimated output is focused into the interferometer by a cylindrical lens oriented vertically. A pump creates a ~1L/min air flow between the mirrors. The cylindrically focused light produces a vertical diameter section of the Fabry-Perot ring pattern that would exit the resonator if the input light were a circular beam. Since only the fringe spacings are necessary, collimating the light into a small line more efficiently uses the laser power than would imaging a full ring pattern on the CCD. A cylindrical mirror focused diverging interferometer output onto the CCD.

The positions of the interference peaks are fitted with a method of least-squares. From this curve fit, angles θ_p are determined, and using (2.10), the fractional order $e(n_i)$ is calculated.

2.1.4 Precautions taken for measurement accuracy, and sources of error

The interferometer's body and mirrors were made of Zerodur. This material's low thermal expansion coefficient, $0.05 \times 10^{-6}/K$, minimizes temperature dependence on the interference pattern.

The curve fit used to find fractional orders is based on Eickhoff and Hall's hypothesis of what the data should look like. It did not include any systematic errors inherent in their experimental apparatus. To account for this problem, Eickhoff and Hall measured fringe location as a function of wavelength for a dye laser with a 320 MHz longitudinal mode spacing. Equation (2.10) shows the relationship between the p th fringe location (expressed in terms of θ_p) and wavelength, λ_0 . Comparing the data to the fit based on (2.10), Eickhoff and Hall found a $\pm 2 \times 10^{-3}$ optical fringe phase measurement error.

Would spherical mirrors help?

Nonparallel mirrors contributed most to the phase measurement error. The resulting interference pattern is a convolution of the Airy disk function seen from an ideal parallel interferometer with a linearly changing interferometer length.

To prevent etalon effects in the interferometer mirrors themselves, the mirror substrates were fabricated with a 15-arcmin wedge. Fringe locations in (2.10) are calculated in terms of the angle θ_p the light exiting the interferometer. The derivation of (2.10) assumes mirrors with parallel substrates, and hence does not account for the distortion of the fringe pattern induced by the wedged substrates. Eickhoff and Hall note that this error is minor, as their measurement errors due to the above factors exceeds the scale of this error.

Other sources of negligible error include expansion or contraction of the interferometer mount and air in the aluminum mirror coatings. As temperature changes, the interferometer mount changes size and hence the mirror spacing. Air in the porous mirror coatings will make the phase change upon reflection temperature dependent. Yet, since these changes occur on a time scale much larger than a measurement, these effects can be ignored.

2.2 Laser with Fixed Wavelength in Air

2.2.1 Theory

Eickhoff and Hall's second method of measuring the refractive index of air was to build a laser with a fixed wavelength in air. A servo connected to the tunable HeNe laser locked the wavelength on the $e = 0$ resonance condition

$$2nd = \lambda_0(m + e). \quad (2-1)$$

The laser cavity is open to the laboratory environment. As the air temperature and pressure changes, the servo continuously changes the laser frequency such that the above condition, defined by a cavity transmission peak, is satisfied. On resonance, the frequency ν satisfies

$$2nd = \lambda_0 m = \frac{c_0}{\nu} m. \quad (2.2-1)$$

As the refractive index n of the air in the laser cavity changes, the laser wavelength in air λ changes to satisfy the resonance condition:

$$2d = \frac{\lambda_0}{n} m = \lambda m. \quad (2.2-2)$$

The refractive index then satisfies

$$n = m \frac{\text{FSR}}{\nu} = m \frac{c}{2d \nu}, \quad (2.2-3)$$

where FSR is the HeNe cavity's free spectral range, c is the speed of light in vacuum, and d is the mechanical length of the cavity.

The laser frequency was measured by heterodyning (interfering) it with a stabilized light source of frequency ν_0 . A high speed rf-photodetector records the beat note at frequency $\Delta\nu = \nu_0 - \nu_{\text{HeNe}}$. A relative index change can be derived from (2.2-3):

$$n_1 = m \frac{\text{FSR}}{\nu_1}, \quad n_2 = m \frac{\text{FSR}}{\nu_2}, \quad \text{and} \quad (2.2-4)$$

$$\Delta\nu_1 = \nu_0 - \nu_1, \quad \Delta\nu_2 = \nu_0 - \nu_2 \quad (2.2-5)$$

Subtracting equations in (2.2-4) and factoring out a ν_1 , (solved for in (2.2-4)), and using (2.2-5) we have

$$n_2 - n_1 = -m \frac{\text{FSR}}{\nu_1} \left(\frac{\nu_1}{\nu_2} + 1 \right) = n_1 \left(\frac{\nu_0 - \Delta\nu_1}{\nu_0 - \Delta\nu_2} + 1 \right). \quad (2.2-6)$$

Putting the term in parenthesis and using the approximation $\nu_0 - \Delta\nu_2 \cong \nu_0$, we have

$$n_2 - n_1 = \frac{n_1}{\nu_0} (\Delta\nu_2 - \Delta\nu_1). \quad [\text{change in air's refractive index}] \quad (2.2-7)$$

2.2.2 Absolute Measurements of Refractive Index

To measure the value of the refractive index of the air in the laser cavity, n_2 , relative to that in vacuum, $n_1 = 1$, we need to know the vacuum laser wavelength λ_0 . As in the Fabry-Perot refractometer case (Section 2.1.2), this can be found by comparison with an I₂-stabilized laser source. Vacuum frequency ν_0 can be calculated from λ_0 and entered into (2.2-7) with $\Delta\nu_1=0$ and $n_1=1$ to determine n_2 .

$$n_2 \cong -\frac{1}{\nu_0} \Delta\nu_2 + 1. \quad (2.2-8)$$

2.2.3 Experimental Setup

Figure 2.2-1 (See Appendix) shows Eickhoff and Hall's experimental setup of the fixed air-wavelength laser. A piezoelectric transducer attached to the HeNe laser tube tunes the laser over its free spectral range. To stabilize the laser frequency, part of the laser beam was steered through an acousto-optic modulator (AOM) and a Fabry-Perot resonator before entering a photodiode. The AOM modulated the frequency at 25 kHz. The photodiode signal and the 25 kHz signal from the modulator were fed into a lock-in

amplifier that generates an error signal received by a servo. The piezo-electric transducer receives the servo signal as its input.

The FP Resonator stabilizes the laser frequency by transmitting only resonator longitudinal frequencies. If the frequency modulated beam did not pass through the resonator before being compared to the 25 kHz modulation, the error signal would be fluctuate according to the HeNe frequency fluctuations. Now consider the system with the resonator in place. When the instantaneous laser frequency is a resonator mode frequency, the transmission is high and the error signal has a specific value Δ . The PZT responds to the error signal by tuning the laser to reproduce the error signal value. Hence, the laser frequency is stabilized to that mode corresponding to the error signal value Δ .

The wavelength-stabilized output is combined with a fixed frequency laser of ν_0 . A high speed photodetector measures the beat frequency $\Delta\nu_2$, from which n_2 is calculated using (2.2-8).

3.0 Edlén's Formula

Edlén's formula is the most accepted method of calculating the refractive index of air. It is a function of their air's temperature, pressure, water vapor content, and CO₂ concentrations. In SI units, Edlén's formula is [Hall, 1997]

$$n - 1 = \frac{D(0.104127 \times 10^{-4})P}{1 + 0.3671 \times 10^{-2}T} - 0.42063 \times 10^{-9}F$$

where

$$D = 0.27651756 \times 10^{-3}[1 + 54 \times 10^{-8}(C - 300)]$$

C = CO₂ content, parts per million

Edlén's Formula (3.1)

P = pressure, Pascals

T = temperature, °C

F = pressure of water vapor, Pascals.

Edlén's formula is a function of air temperature, and content of molecules in the air, expressed in terms of concentration or pressure. Temperature, pressure, and concentration are related through the Ideal Gas Law:

$$pV = nRT, \text{ where}$$

p is gas pressure, Pascals
 V is gas volume, m^3
 n is the number of moles
 $R = 8.31 \text{ J/mol} \cdot \text{K}$, gas constant
 T is the gas temperature, K.

3.1 The Lorentz-Lorenz formula (a.k.a. the Claussius-Mossotti Equation)

The Lorentz-Lorenz formula states a relationship between the above properties of a gas and its refractive index. Edlén's formula is based upon this relationship. Pressures, temperatures, and concentrations of CO_2 , H_2O in air are measured, and their contribution to the refractive index is calculated with this formula.* Its derivation follows, and is valid for non-polar molecules in an isotropic media, such as air [2],[9].

The relationship between a molecule's electric dipole moment, \vec{p} , and the effective field, \vec{E} , e.g., from a photon, is

$$\vec{p} = \alpha \vec{E}, \quad (3.1-1)$$

where α is the molecule's *mean polarizability*, and

$$\vec{E} = \vec{E} + \frac{1}{3\epsilon_0} \vec{P} \quad \text{[Effective Field]} \quad (3.1-2)$$

where ϵ_0 is the permittivity of free space ($=10^9/36\pi$ coulomb²/Joule), and \vec{E} applied macroscopic field. The macroscopic field is a statistical average of the electric field in a region containing many molecules. The effective field exerts a force on a single molecule.

If the air has N molecules per unit volume of mean polarizability \vec{p} , then the total electric moment \vec{P} per unit volume is

$$\vec{P} = N\vec{p} = N\alpha \vec{E}. \quad (3.1-3)$$

From (3.1-2) and (3.1-3), we have

$$\vec{P} = N\alpha \left(\vec{E} + \frac{1}{3\epsilon_0} \vec{P} \right) \quad (3.1-4)$$

* This explanation is offered to ground the formula in physics the author can relate to. Most of the literature on Edlén's formula involves modifications of the coefficients, and not an analysis of its conceptual basis.

Recall that

$$\vec{P} = \chi \vec{E} = (\epsilon - \epsilon_0) \vec{E} = (K - 1) \epsilon_0 \vec{E} \quad (3.1-5)$$

where χ is the unitless electric susceptibility, and

$$K = \frac{\epsilon}{\epsilon_0} = n^2 \quad (3.1-6)$$

is the dielectric constant. Substituting (3.1-5) into (3.1-4) and expressing K in terms of the refractive index, we have

$$\alpha = \frac{3\epsilon_0}{N} \frac{(n^2 - 1)}{(n^2 + 2)} \quad \begin{array}{l} \text{The Lorentz-Lorentz formula or} \\ \text{Clausius-Mossotti equation} \end{array} \quad (3.1-7)$$

This equation describes the contribution of a molecule with a mean polarizability α with a concentration $N \text{ m}^{-3}$ to the refractive index n of air. According to the CRC Handbook of Chemistry and Physics [6], the mean polarizability of H_2O and CO_2 are $1.45 \times 10^{-24} \text{ cm}^3$ and $2.911 \times 10^{-24} \text{ cm}^3$ respectively. Yet, (3.1-7) shows that $[\alpha] = [\epsilon_0] \times \text{Volume}$.

So the quantities listed in the CRC must be $\frac{\alpha}{\epsilon_0}$.

4.0 Comparison of index measurements with Edlén's formula predictions

Figure 4.1 shows the results of Eickhoff and Hall's measurements, and Figure 4.2 the accompanying pressure, temperature, and pressure measurements.

Note that Edlén's formula responds to the fast temperature changes at ≈ 15 and ≈ 25 hours while the two experimental measurements do not. Eickhoff and Hall attribute this to the inability of the temperature inside the resonator and the open cavity laser to change as fast as the ambient air. This makes sense to me for the resonator, as it's a closed structure with air being pumped through it. Yet, the open cavity laser does not trap the air as much as the FP resonator. I'd expect to see some correlation with its refractive index readings and fast temperature changes. Eickhoff and Hall cite this is an advantage of the fixed-air wavelength laser.

Eickhoff and Hall cite water adsorption in the MgF_2/Al resonator mirror coatings as the cause of the offset of the FP resonator index measurement between 30 and 40 hours and 75 to 85 hours. The other apparatus used pure dielectric mirrors and did not have this offset. Surely this is a correlation, but I do not see the causation. Why is the offset apparent only when Δn_{air} has a relatively small slope?

The answer, the researchers say, arises from

1. the thermal mass time delay (coefficient of thermal expansion) of the experimental components.
2. the experiment began during a time of fast index change. Had $t = 0$ been moved to 40 hours, the offsets would occur during the high slope regions.

Consider the case proposed in 2. When the index begins to change rapidly, the interferometers, because of the time delay, would record index changes offset from the Edlén's formula prediction. In the case where the experiment began during a high slope period, the time delay of the interferometer components had already finished. The time delay manifested itself when the slope leveled off.

Agreement among the three readings is $\approx 1 \times 10^{-7}$ for the >80 measurement time. For a ten hour period, the agreement is less than 5×10^{-8} .

5.0 Conclusions

Figure 4.1 shows that the refractive index changes by at most 4×10^{-6} over a three day period. How would this change effect an optical path difference measured by an interferometer used in Lucent's Scalpel lithography system?

The longer the interferometer arms are, the more air's refractive index will affect OPD measurements. Assuming both arms are in air, we will consider local changes in n_{air} in one arm and how it affects the OPD between the arms. Since $OPD = n_{\text{air}}\Delta$, where Δ is the vacuum optical path difference, $\partial(OPD) = \partial n_{\text{air}}\Delta$. For

$$\begin{aligned}\partial(OPD) &= 2.5 \text{ nm}, \\ \partial n_{\text{air}} &= 4 \times 10^{-6},\end{aligned}$$

$$\Delta = \frac{\partial(OPD)}{\partial n_{\text{air}}} \approx 1 \text{ mm}.$$

So for a 4×10^{-6} local change in n_{air} , the optical path difference between the arms of the interferometer will change by 2.5 nm for a vacuum OPD of 1 mm. To prevent this error, the interferometer arms must be shorter than 1 mm long. The longer the arms, the more the changes in index affect OPD. Clearly this is not easy to do, and makes the tracking of refractive index necessary.

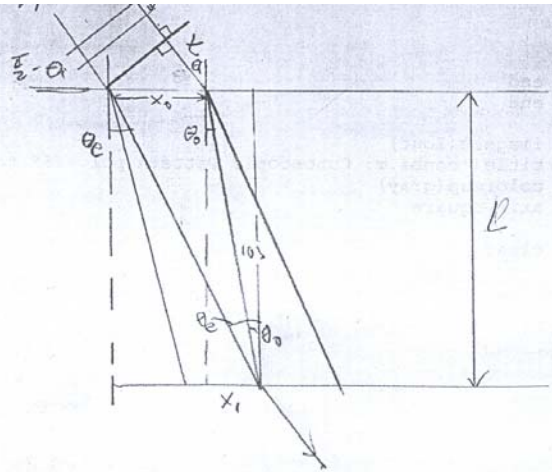
Of course, one might ask if the chip manufacturers place their interferometers in a vacuum system. After all, if electron beam lithography is being used, the e-beams require a vacuum [10]. Why not place the interferometers in it?

6.0 References

- [1] B. Edlén, "The Refractive Index of Air," *Metrologia* **2**, 71-80 (1966).
- [2] M. Born and E. Wolf, *Principles of Optics*, 6th ed. (Pergamon, New York, 1980).
- [3] M. Eickhoff and J. Hall, "Real-time precision refractometry: new approaches," *Applied Optics* **36**, 1223-1234, (1997).
- [3a] J. Hall, personal communication, November 29, 1999.
- [4] A. Hand, "Photonics Will Assist Next Lithography Tool." *Photonics Spectra*, 92-99, December 1998.
- [5] W. Lichten, "Precise wavelength measurements and optical phase shifts II. Applications," *J. Opt. Soc. Am. A* **3**, 909-915 (1986).
- [6] D.R. Lide, Editor, *CRC Handbook of Chemistry and Physics*, 80th ed (CRC Press, 1999)
- [7] Miller, David, presentation on Optical Interconnects, JILA, November 1, 1999.
- [8] J.C. Owens, "Optical Refractive Index of Air: Dependence on Pressure, Temperature, and Composition," *Applied Optics* **6**, 51-59, (1967).
- [9] J. Reitz, F. Milford, and R. Christy, *Foundations of Electromagnetic Theory*, Fourth Edition (Addison-Wesley, New York, 1993).
- [10] Wagner, K., personal communication.
- [11] A.J. Wallard, "The frequency stabilization of gas lasers," *Journal of Physics E: Scientific Instruments* **6**, 793-807 (1973).

Appendices

Appendix Phase Change Across A medium



B1: wavefront section 1

B2: wavefront section 2

B2 travels a distance t more than B1 before hitting surface

From diagram, $t = x_0 \sin \theta_i$

10) travels distance $d_0 = L / \cos \theta_e$

1e) travels distance $d_e = L / \cos \theta_e$

Phase Change in Media

$$\phi_0 = k d_0 = \frac{2\pi}{\lambda} \frac{L n_0}{\cos \theta_0}$$

$$\phi_e = k d_e = \frac{2\pi}{\lambda} \frac{L n_e(\theta_e)}{\cos \theta_e}$$

$$x_1 = d_0 \sin \theta_0 = L \tan \theta_0$$

$$x_1 + x_0 = d_e \sin \theta_e = L \tan \theta_e$$

$$x_0 = L \tan \theta_e - x_1 = L \tan \theta_e - L \tan \theta_0 = L (\tan \theta_e - \tan \theta_0)$$

$$\text{So } t = x_0 \sin \theta_i = L (\tan \theta_e - \tan \theta_0) \sin \theta_i$$

So total phase change is

$$\delta = \phi_0 - \phi_e + n_e k t = \frac{2\pi L}{\lambda} \left(\frac{n_0}{\cos \theta_0} - \frac{n_e(\theta_e)}{\cos \theta_e} + (\tan \theta_e - \tan \theta_0) \sin \theta_i \right)$$

From Snell's Law:

$$\sin \theta_0 = \frac{\sin \theta_i}{n_0}, \quad \sin \theta_e = \frac{\sin \theta_i}{n_e(\theta_e)}$$

$$\delta = \frac{2\pi L}{\lambda} \left(\frac{1}{\cos \theta_0} (n_0 - \sin \theta_0 \sin \theta_i) + \frac{1}{\cos \theta_e} (-n_e(\theta_e) + \sin \theta_e \sin \theta_i) \right)$$

$$\delta = \frac{2\pi L}{\lambda} \left[\frac{1}{\cos \theta_0} (n_0 - n_0 \sin^2 \theta_0) + \frac{1}{\cos \theta_e} (-n_e(\theta_e) + n_e \sin^2 \theta_e) \right]$$

$$\delta = \frac{2\pi L}{\lambda} \left[\frac{n_0}{\cos \theta_0} \cos^2 \theta_0 - \frac{n_e(\theta_e)}{\cos \theta_e} \cos^2 \theta_e \right] = \frac{2\pi L}{\lambda} \left[n_0 \cos \theta_0 - n_e(\theta_e) \cos \theta_e \right]$$

Phase Change δ

$$(10) \quad \delta_n = \frac{2\pi L}{\lambda} n_n \cos \theta_n$$

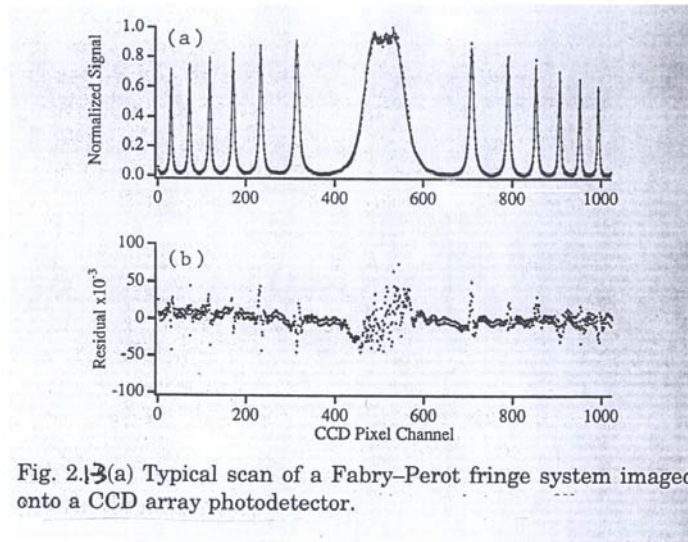


Fig. 2.13(a) Typical scan of a Fabry-Perot fringe system imaged onto a CCD array photodetector.

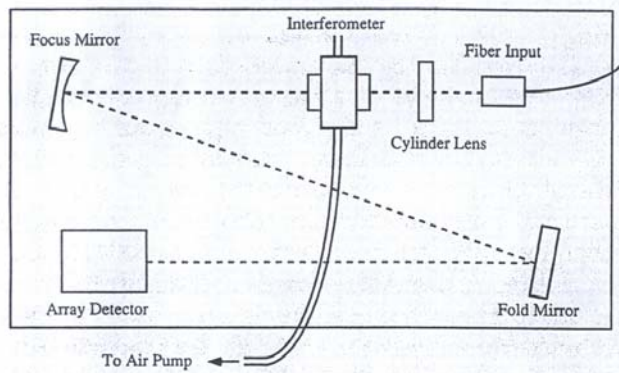
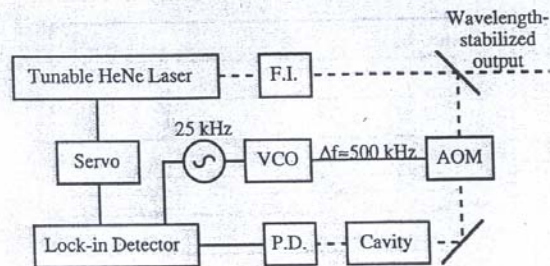
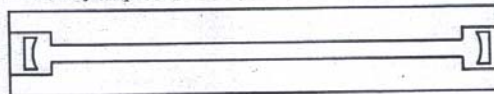


Fig. 2.13 Layout of the Fabry-Perot refractometer. Collimated output from the fiber coupler is converged in the vertical plane before entering the plane-plane Fabry-Perot interferometer. As discussed in text, the direction of fringes and the CCD detector line are perpendicular to the plane of the figure to eliminate astigmatism. Curvature of the $R = 100\text{-cm}$ focusing mirror is exaggerated for clarity.

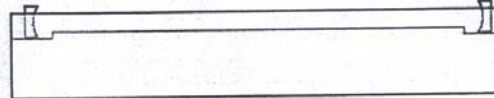


(a)

Air Cavity: Top View



Air Cavity: Side View



(b)

Fig. 2.2-1 (a) Layout of the air-wavelength standard prototype: F.I., Faraday isolator; P.D., photodetector; AOM, acousto-optic modulator that is driven by a voltage-controlled oscillator (VCO). Analog 25-kHz applied voltage generates ± 500 -kHz FM excursion of the 80-MHz output, enabling phase-sensitive detection of lock signal. Note that the laser output is unmodulated and has a constant wavelength measured in laboratory air. (b) Sketch of top and side views of the Zerodur bar cavity that was used in the constant-air-wavelength standard prototype. Curvature of the mirrors is exaggerated for clarity. Mating surfaces are tinned individually with indium solder before the mirrors are attached firmly with indium solder flowed onto the cylindrical surface.

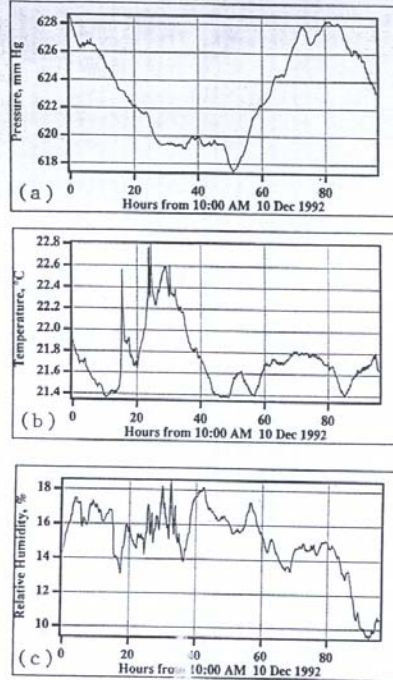


Fig. 4.2 Output of the weather bureau showing (a) ambient pressure, (b) temperature, (c) relative humidity as functions of time.

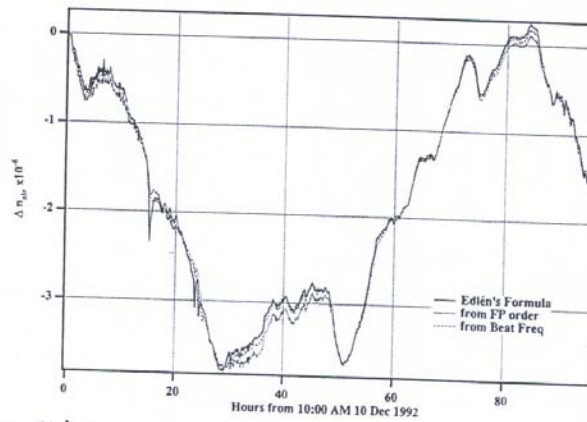


Fig. 4.1 Comparison of the refractometers. The change in the index of refraction of the ambient air is shown as a function of time. Output from each refractometer is plotted on the same axis from 0 at $t = 0$. Agreement for index changes is $\pm 5 \times 10^{-8}$ for some hours and $\approx \pm 1 \times 10^{-7}$ for the entire run. Accidental choice of starting time during epoch of rapid change leads to apparent offset $\approx 1 \times 10^{-7}$ during quiescent times. FP, Fabry-Pérot.